

# Water Conservation & Management (WCM)

DOI: http://doi.org/10.26480/wcm.02.2024.171.178



ISSN: 2523-5672 (Online) CODEN: WCMABD RESEARCH ARTICLE

# ESTIMATION THE WATER RATIO INDEX (WRI) AND AUTOMATED WATER EXTRACTION INDEX (AWEI) OF BATH IN THE UNITED KINGDOM USING REMOTE SENSING TECHNOLOGY OF THE MULTISPECTRAL DATA OF LANDSAT 8-OLI

Hayder H. Kareema\*, Muammar H. Attaeeb, Zainab Ali Omranc

- a Structures and Water Resources Engineering Department, Faculty of Engineering, University of Kufa, Al-Najaf, Iraq
- <sup>b</sup> Department of Civil Engineering, College of Engineering, University of Misan, Misan, Amarah 62001, Iraq
- <sup>c</sup> Department of Civil Engineering, Faculty of Engineering, University of Babylon, Babil, Iraq
- \*Corresponding Author's E-Mail: hayderh.alshaibani@uokufa.edu.iq

This is an open access journal distributed under the Creative Commons Attribution License CC BY 4.0, which permits unrestricted use, distribution, and reproduction in any medium, provided the original work is properly cited

### **ARTICLE DETAILS**

### Article History:

Received 23 September 2023 Revised 26 October 2023 Accepted 24 November 2023 Available online 30 November 2023

### **ABSTRACT**

Remote sensing is commonly utilized for surface cover classification and change analysis. An important approach in studying water resources and assessing hydrological drought involves utilizing remote sensing to extract various land cover features. Given the potential influence of environmental noise, the objective of this study is to devise an index that enhances water extraction accuracy while establishing a stable threshold value. The investigation focuses on the Water Ratio Index (WRI) and the Automated Water Extraction Index (AWEI) in the context of Bath, United Kingdom, particularly addressing areas with shadows and dark surfaces that often lead to misclassifications by other indices. The application and comparative performance assessment of these indices are conducted using GIS and Remote Sensing technology. WRI analysis reveals index values ranging from 0.83 to 1.24, highlighting regions with water or moisture content (WRI greater than 1) and extensive areas devoid of water (WRI less than 1). Notably, AWEI nsh yields more accurate predictions than AWEI sh, which tends to identify shade and man-made surfaces rather than water surfaces. AWEI nsh exhibits a significantly higher water land cover figure (11342.5) compared to AWEI sh's minimal value (359.5). In scenarios where water information is susceptible to noise, AWEI proves to be a more suitable and effective alternative water index. It is recommended for use in locations with challenging water data, offering improved accuracy and reliability.

# KEYWORDS

WRI, AWEI, Remote Sensing Technology, Bath, United Kingdom.

### 1. Introduction

Scientists from various disciplines are currently investigating the impacts of environmental changes on both natural ecosystems and human societies. Alterations in land use/cover (LULC), climate, and other environmental factors have had widespread consequences across the globe, with surface water being a fundamental Earth resource undergoing dynamic transformations over time and space. Extensive research has been dedicated to comprehending the ecological, health, social, and economic repercussions resulting from shifts in surface water (Bond et al., 2008; Alderman et al., 2012; Li et al., 2012; Sun et al., 2012). Disasters like floods, the proliferation of waterborne diseases, and shortages of water in arid tropical regions often trace back to alterations in surface water levels. Consequently, it is of utmost importance to actively monitor and promptly share data on surface water dynamics to facilitate informed decisionmaking and the implementation of effective remedial actions (Giardino et al., 2010).

Recent years have witnessed transformations in land cover and land use on Earth. Numerous studies underscore the significance of recognizing these shifts, such as those between agriculture, forested areas, urban expanses, and water bodies. However, detecting these changes, especially when they occur on a smaller scale, can be challenging due to their gradual nature. Long-term historical data plays a pivotal role in equipping

scientists with concrete information to identify, explain, and mitigate these transformations.

Surface water (SW) is an indispensable resource that significantly influences everyday life. Its versatile applications encompass consumption, agricultural irrigation, aquaculture, and thermoelectric cooling. Variations in surface water patterns serve as valuable indicators of environmental, climatic, and human-induced alterations in land cover. From a strategic perspective, SW stands as a crucial asset for human wellbeing and societal advancement (Ahmed et al., 2017). It plays a vital role in sustaining human populations, agricultural productivity, and ecosystems (Lu et al., 2011). Notably, drinkable water sources include precipitation, groundwater, and a variety of surface water bodies like rivers, ponds, and lakes (Mueller et al., 2016). Therefore, precise extraction of surface water regions is pivotal (Elsahabi et al., 2016). Accurate mapping of surface water holds paramount importance for both academic study and policy formulation, providing insights into its spatial and temporal distribution (National Researcher Council, 2008). Changes in water levels are often identified through the extraction of water-related features from multiple satellite images, followed by comparative analysis to detect discrepancies (Du et al., 2012).

Water indices represent a relatively novel technique for detecting shifts in aquatic ecosystems. Compared to classification-based approaches, index-

Quick Response Code

Access this article online



Website: www.watconman.org DOI:

10.26480/wcm.02.2024.171.178

based algorithms offer advantages in terms of accuracy, speed, simplicity, and their ability to function without prior information (Li et al., 2013). Diverse algorithms for extracting water from satellite imagery have been developed and applied. Statistical pattern recognition methods encompass both unsupervised classification methods that identify endmembers and supervised techniques that employ ground truth data (Li et al., 20132; Nath and Deb, 2010; Sivanpillai and Miller, 2010; Karpatne et al., 2016; Tulbure and Broich, 2013; Acharya et al., 2016). Among these, index-based approaches are commonly employed for assessing surface water, utilizing threshold values to distinguish water from the background. Examples of such indices include the Normalized Difference Water Index (NDWI), the Modified Normalized Difference Water Index (MNDWI), the Water Ratio Index (WRI), and the Normalized Difference Vegetation Index (NDVI) (McFeeters, 1996; Xu, 2006; Shen and Li, 2010; Rouse et al., 1973). However, challenges arise in setting appropriate thresholds for various conditions, such as shading, topography, forests, urban areas, and coastlines (Acharya et al., 2017).

In the field of natural resource management and environmental assessment, remote sensing has rapidly advanced. Utilizing space-based technology, remote sensing enables frequent and accurate updates to surface water maps. The adoption of remote sensing has greatly improved the analysis and sharing of information concerning alterations in diverse natural resources, placing particular emphasis on surface water. Utilizing remote sensing in conjunction with geographic information systems (GIS) allows for monitoring current conditions and spatiotemporal changes in rivers, lakes, reservoirs, and other surface water features. Remote sensing plays a crucial role not only in regions lacking field data and detailed maps but also as a cost-effective alternative for detecting features and understanding hydrogeological systems in well-mapped areas (Peng et al., 2022).

Its applications span diverse domains, encompassing flood risk assessment, damage mitigation, water resource management, analysis of surface water availability variations, water quality monitoring and assessment, and the study of water-related disease epidemiology (Dewan et al., 2007; Ji et al., 2009; Proud et al., 2011; Prigent et al., 2012; He et al., 2012; Guttler et al., 2013). Information on surface water is extracted and analyzed using satellite sensors with varying spatial, temporal, and spectral resolutions. Among these sensors, Landsat satellites are extensively employed in surface water and environmental studies, often serving as a foundational step in processing remotely sensed data. Commonly utilized optical imaging water classification techniques can be categorized into four main groups: thematic classification, linear unmixing, single-band thresholding, and two-band spectral water indices (Dambach et al., 2012; Lira, 2006; Sethre et al., 2005; Jain et al., 2005; Jain et al., 2006). Combining multiple approaches has also been proposed to enhance the precision of water extraction (Jiang et al., 2012; Verpoorter et al., 2012; Ryu et al., 2002). Notable examples of such efforts include studies (Jiang et al., 2012; Sun et al., 2012; Verpoorter et al., 2012).

Water index algorithms play a prominent role in detecting water features due to their simplicity, computational efficiency, and capacity to perform well even in the presence of certain noise. These algorithms have demonstrated excellent outcomes when applied to Landsat imagery. Prominent among them are multiband water index techniques like the Water Ratio Index (WRI) and the Automated Water Extraction Index (AWEI) (Tri et al., 2016).

In innumerable ways, surface water is an essential natural force. In order to effectively manage and conserve this precious resource, it is crucial to get an appreciation for their far-reaching effects. We can build a more sustainable and resilient future for human societies and the natural world by learning about the importance of surface water and the impacts of hydrological climate changes that have led to its significant scarcity and decline. This study aims to analyse the hydrological data for Bath, UK, with the objective of understanding how surface water has responded to shifts in climate and/or human activities. Additionally, it seeks to evaluate the effectiveness of widely used water indices by employing time series Landsat data to gauge their ability to capture variations in surface water distribution.

# 2. BATH STUDY AREA

Bath, situated in the ceremonial county of Somerset, England, is renowned for its historic Roman baths. Its population was recorded at 101,557 during the 2021 census. Nestled in the valley of the River Avon, Bath is easily accessible, lying approximately 156 kilometers west of London and 11 kilometers southeast of Bristol. The city holds significant historical value, being designated a World Heritage Site for its ancient Roman baths since 1987, and subsequently added to the transnational World Heritage

Site of "Great Spa Towns of Europe" in 2021. Bath serves as the county seat of Somerset and is its largest city (100 Largest Cities and Towns in the UK by population, 2019). It is covering an area of 28 square kilometers (11 square miles), Bath features an iron bridge traversing a lake, while a yellow stone structure stands in the distance. Trees on the left extend towards the shoreline. Noteworthy is the cast-iron bridge at Sydney Gardens, spanning the Kennet and Avon Canal, adjacent to Cleveland House (Published Contaminated Land Inspection of the area surrounding Bath, 2023). Another natural highlight is Kensington Meadows, a riverside stretch with a mix of wooded and open spaces, designated as a local nature reserve. The geothermal springs that supply the Roman baths are fed by rainwater originating from the Mendip Hills. Geothermal energy forces hot water upward through fissures and faults in the limestone. Daily, 1,170,000 liters of hot water, at 46 °C, gush from the Pennyquick geological fracture (Kensington Meadows, 2016).

Bath experiences a climate typical of the broader Southwest of England, characterized by mildness and frequent rainfall. The annual average temperature hovers around 10 degrees Celsius. The presence of the nearby ocean tempers seasonal temperature fluctuations compared to the rest of the UK. July and August are the warmest months, with mean daily maxima around 21 °C. Winters bring lows of 1 to 2 degrees Celsius. The region benefits from the Azores high pressure during summer, yielding pleasant weather, although inland convective clouds can limit sunshine. Bath records fewer sunny days per year compared to the regional average of 1,600. Precipitation, approximately 700 millimetres annually, is influenced by Atlantic depressions and convective activity. These factors contribute to a higher percentage of summer precipitation, often triggered by ground heating leading to showers and thunderstorms. Snowfall, spanning 8 to 15 days, is relatively common during winter. The strongest average wind speeds occur from November to March, predominantly from the southwest (South West England, 2006). Figures 1 and 2 provide visual representations of Bath's Digital Elevation Model (DEM) and a 3dimensional portrayal of its surface land elevations.

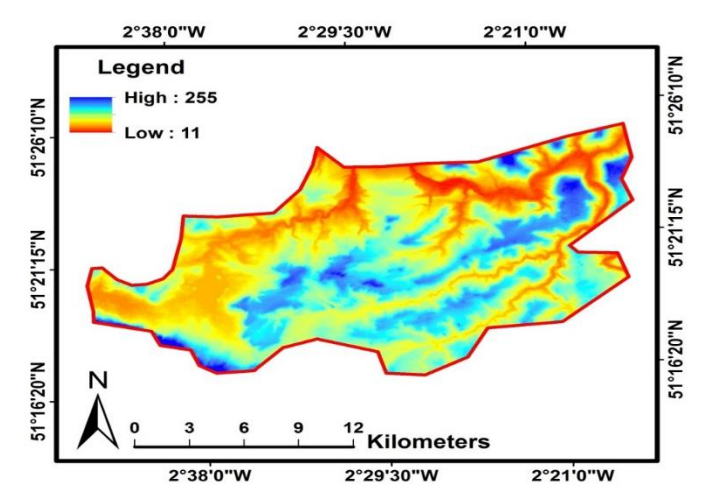


Figure 1: Digital Elevation Model (DEM) of Bath in the UK.

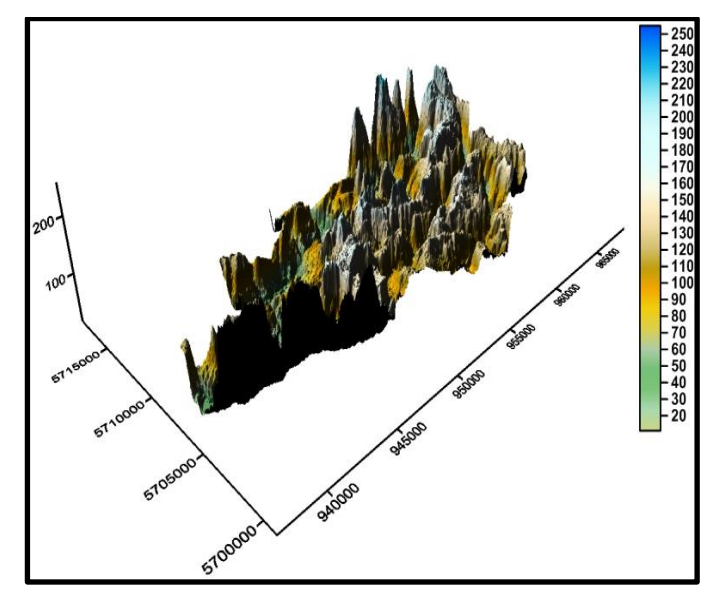


Figure 2: 3-Dimensional view of Bath ground surface elevations.

### 3. REMOTE SENSING METHODOLOGY

In contrast to direct, on-site observation, remote sensing involves collecting data about an object or phenomenon from a distance. This term commonly applies to data collection about Earth and other celestial bodies within the solar system. Remote sensing finds utility in various fields like geophysics, geography, and land surveying, as well as across multiple branches of Earth science. In modern usage, "remote sensing" typically refers to gathering information about Earth's surface using sensors aboard satellites or aircraft. Signals, such as electromagnetic radiation, travel through space, reaching both the Earth's oceans and its atmospheric layers. When a signal is emitted from a satellite or aircraft and its reflection is captured by a sensor, this constitutes "active" remote sensing. In contrast, "passive" remote sensing occurs when an object is illuminated by sunlight, and the radiation emitted or reflected from the object is collected by a sensor. Passive sensors often measure radiation from reflected sunlight. In active remote sensing, energy is actively transmitted to scan objects and spaces, and the sensor captures the reflected or backscattered radiation. Active techniques like radio detection and ranging (RADAR) and light detection and ranging (LiDAR) utilize the time delay between signal emission and reception to determine an object's position, velocity, and direction.

Utilizing satellite imagery from Landsat 8 OLT/TIRS, this study establishes a comprehensive system for mapping and monitoring water bodies. The process encompasses data collection, image preprocessing, calculation of spectral water indices, derivation of surface water indices, and the successful fulfillment of the paper's objective. The L1T data sourced from USGS Landsat imagery are geographically aligned and referenced to the UTM (zone 29 N) coordinate system using the WGS 84 datum, presented in GeoTIFF format (Gautam et al., 2015). The Landsat images encompass a variety of land cover types, including water, forests, non-forest vegetation, bright and dark soil, brown soil, bright built areas, asphalt, dark constructed areas, and shadows. To delve deeper into the influence of different land cover types on water extraction accuracy, an analysis of spectral data from these pristine pixels was conducted. The Water Reflectance Index (WRI) and Automated Water Extraction Index (AWEI) are both formulated by combining data from four spectral bands of Landsat 8 OLI, enhancing the differentiation between water and darker surfaces (Shen and Li, 2010; Feyisa et al., 2014). The WRI and AWEI are devised to optimize the distinction between water and non-water regions through band differencing, addition, and the application of specific coefficients. Consequently, three distinct equations (Eqs. (1), (2), and (3) are presented to achieve a more precise extraction of surface water while effectively suppressing non-water pixels.

$$WRI = \frac{B_{Green} + B_{Red}}{B_{NIR} + B_{SWIR1}} \tag{1}$$

$$AWEI_{nsh} = 4(B_{Green} - B_{SWIR1}) - (0.25B_{NIR} + 2.75B_{SWIR2})$$
 (2)

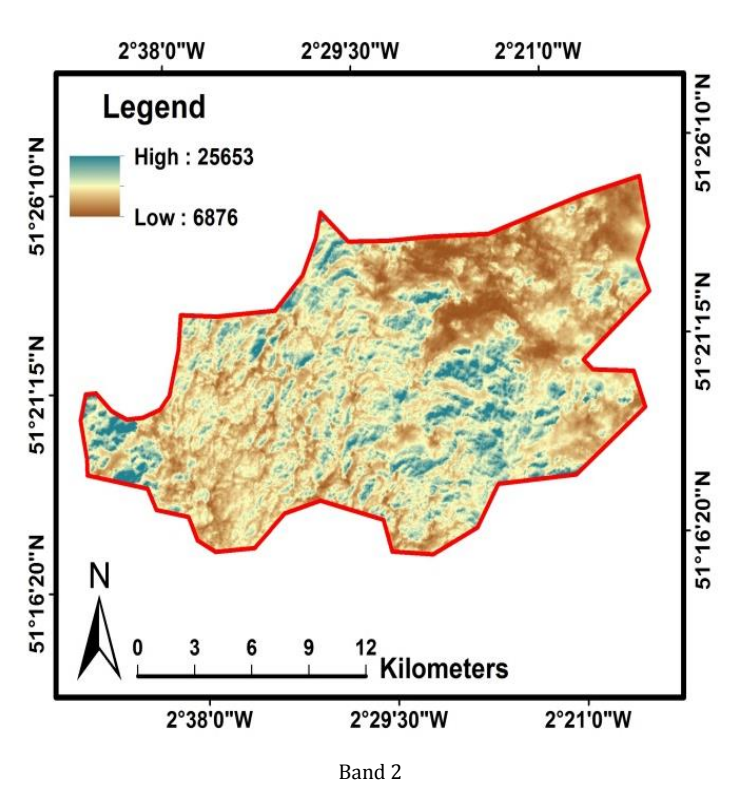
$$AWEI_{sh} = B_{Blue} + 2.5B_{Green} - 1.5(B_{NIR} + B_{SWIR1}) - 0.25B_{SWIR2}$$
 (3)

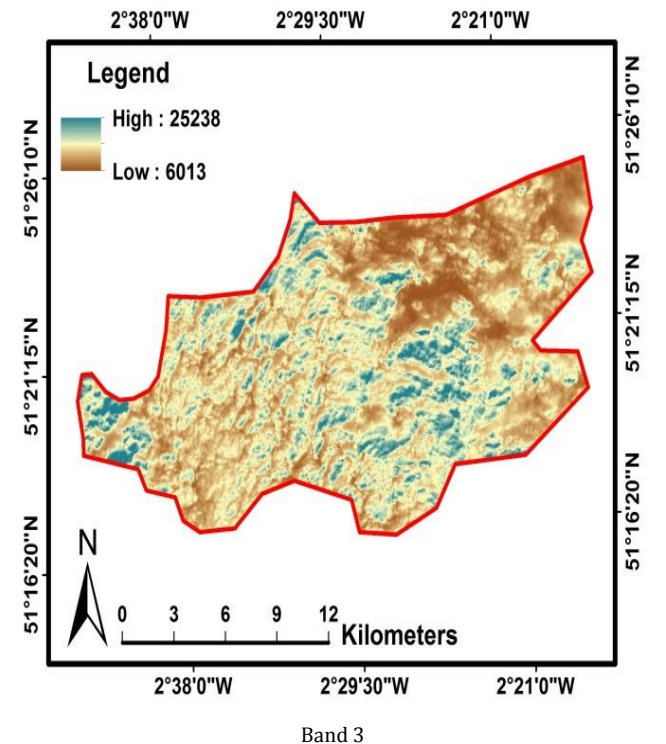
Where: where B is the reflectance value of spectral bands of Landsat 8 OLI: Band 2 (Blue), Band 3 (Green), Band 4 (Red), Band 5 Near Infrared (NIR), Band 6 Shortwave Infrared (SWIR1) and Band 7 Shortwave Infrared (SWIR2).

The AWEI nsh index is designed to effectively exclude non-water pixels, like dark building surfaces in urban contexts. AWEI sh, on the other hand, primarily aims to improve accuracy by eliminating shadow pixels that AWEI nsh might miss. Eq. (2) is optimized for situations where shadows have minimal impact, indicated by the "nsh" subscript, while Eq. (3) is tailored to enhance water extraction precision in regions with shadows or other dark surfaces, denoted by the "sh" subscript. However, Eq. (3) may inadvertently misidentify highly reflective materials like ice, snow, and reflective rooftops as water.

Analysis of reflectance properties across various land cover types informs the coefficients used in Eqs. (2) and (3), as well as the sums of bands within the specified spectrum. These coefficients are empirically determined based on reflectance patterns observed across a dataset of pure pixels representing different land cover types. To ensure water and non-water surfaces with low reflectance are distinct, an iterative approach is employed to find optimal coefficient values. Rounding coefficients enhances user-friendliness. By constraining non-water pixels to values below 0 and water pixels to values above 0, this coefficient selection not only improves the differentiation of water pixels from others but also stabilizes the threshold for identifying water.

To directly extract water index values (WRI, AWEI nsh, and AWEI sh) for Bath, UK, the relevant bands representing the study area must be obtained. Using ArcMap software, the study region's boundaries are extracted by processing Landsat 8 OLI images for the necessary bands to implement Eqs. 1, 2, and 3. Figure 3 depicts the extracted bands for the study area.





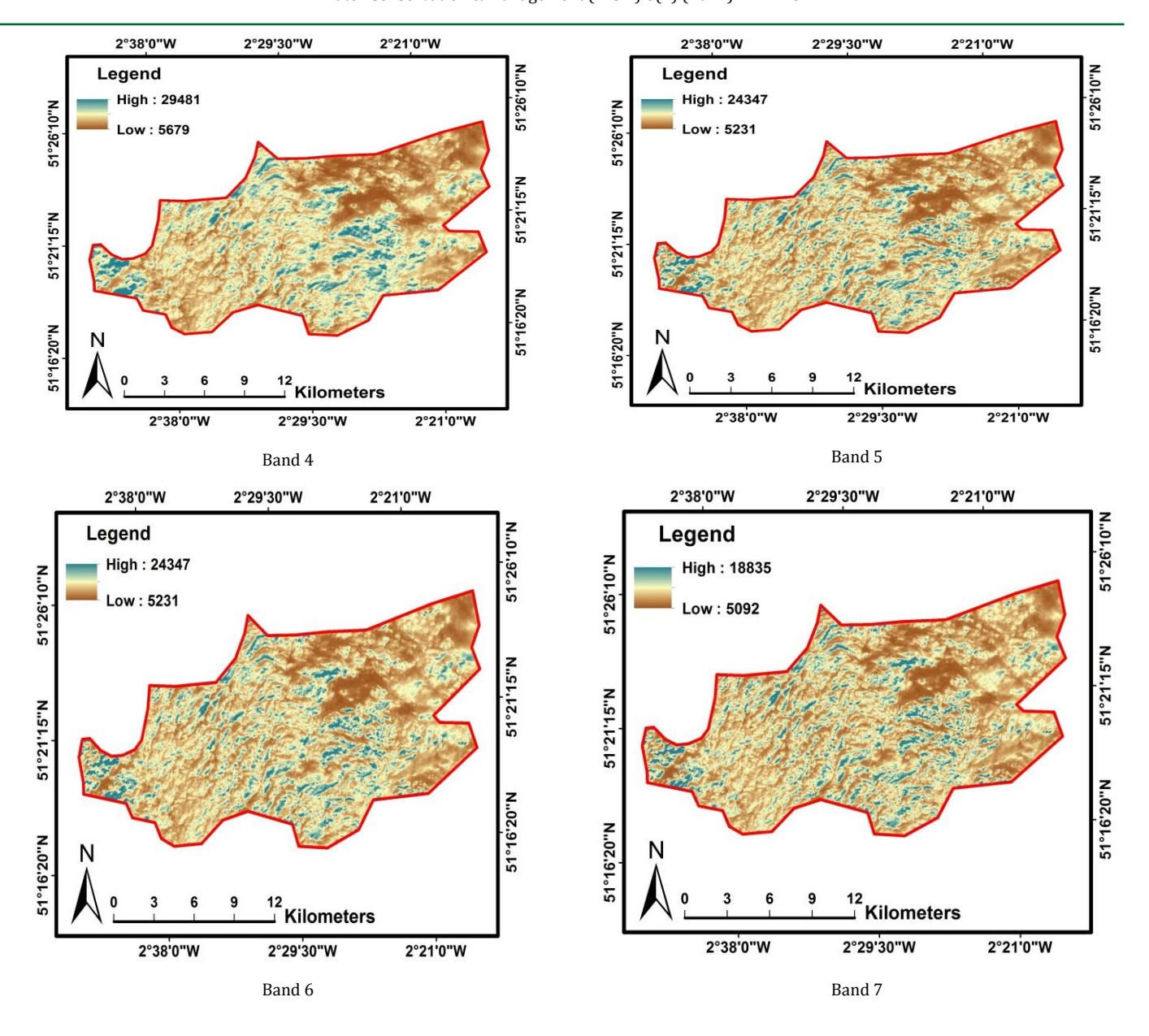
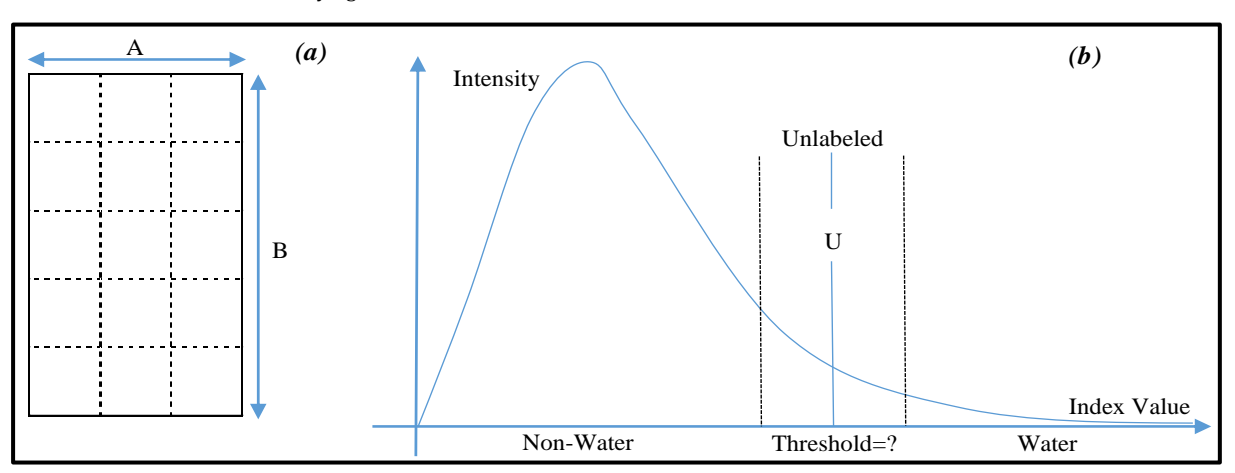


Figure 3: Landsat 8 OLI bands: a) Band 2 (Blue), b) Band 3 (Green), c) Band 4 (Red), d) Band 5 Near Infrared (NIR), e) Band 6 Shortwave Infrared (SWIR1) and f) Band 7 Shortwave Infrared (SWIR2)

## 4. RESULTS AND DISCUSSION

In this study, insights into the evolution of Bath and the driving factors behind it were gained through satellite image analysis. The purpose was to develop scientific measures to mitigate potential future drought disasters. The split-based approach (SBA) was employed to analyze local threshold variations in scene data for classifying "water" and "nonwater".

The global limitation threshold between these categories was heightened through this procedure, as illustrated in Fig. 4. Utilizing the geospatial analysis method, originally termed smart quantile, enabled the identification of the demarcation between water and nonwater classes in the processed images of Landsat 8-OLI.



**Figure 4:** Portrays the Split-Based Approach (SBA): (a) Depiction of the SBA applied to the scene image, and (b) Visual representation depicting the pixel value distribution for the two categories, namely water (As utilized by 46).

The evaluation of the reliability and accuracy of threshold enhancements for WRI and AWEI was performed through a visual method. This visual approach entailed a comparison of the appearance of objects in Landsat 8 images with the classification results obtained from various thresholds, including equal interval, quantile, geometrical interval, and natural break.

The Water Ratio Index (WRI) stands as a crucial and widely acknowledged metric employed for the evaluation and administration of water resources across diverse contexts. Serving as a quantitative measure, WRI aids in assessing the efficacy of water utilization within specific regions, sectors, or processes. It furnishes valuable insights into the equilibrium between water availability and demand, empowering decision-makers to make well-informed choices regarding water management, conservation, and sustainable development. The fundamental concept of the Water Ratio Index revolves around comparing the amount of water consumed or withdrawn for a particular task, activity, or outcome with the existing water resources. On a parallel note, the Automated Water Extraction Index (AWEI) emerges as a specialized remote sensing and geospatial tool designed for monitoring and evaluating water availability and vegetation health, particularly in arid and semi-arid regions. AWEI harnesses satellite imagery and computational algorithms to extract meaningful insights about the presence and distribution of water resources and vegetation cover. This information proves invaluable for water resource management, environmental monitoring, and land use

Developed as a strategic response to the challenges posed by water scarcity and the imperative for efficient water resource management, AWEI presents a systematic approach to analyze and interpret satellite data for quantifying water-related parameters.

Water index values were calculated and extensively presented in Figures 5, 6, and 7 for comparative purposes. Land and water surface areas were quantified using various indices in the examined regions. Outputs of water extraction from Landsat 8-OLI images are displayed in Figures 5, 6, and 7. Upon visual inspection of Figure 6, it became evident that AWEI yielded more accurate surface water mapping than WRI, particularly in suppressing shadow and nonwater surfaces as compared with Figure 5. In most cases, WRI yielded noisy results. However, at a test site in Bath, Figures 6 and 7 showed minimal discrepancies between AWEI outcomes. The visual examination of classification results indicated that AWEI was effective in extracting surface water in the presence of shadow and urban surfaces. In Bath, where significant shadow surfaces were absent, both AWEI sh and WRI produced visually accurate outputs. Overall, the visual inspection clearly demonstrated that AWEI sh outperformed AWEI nsh in effectively suppressing shadowed surfaces. The outputs can be used to generate quantitative values or visual representations that help researchers, policymakers, and stakeholders make informed decisions. The formula and algorithm for AWEI computation may vary based on specific research goals and study areas.

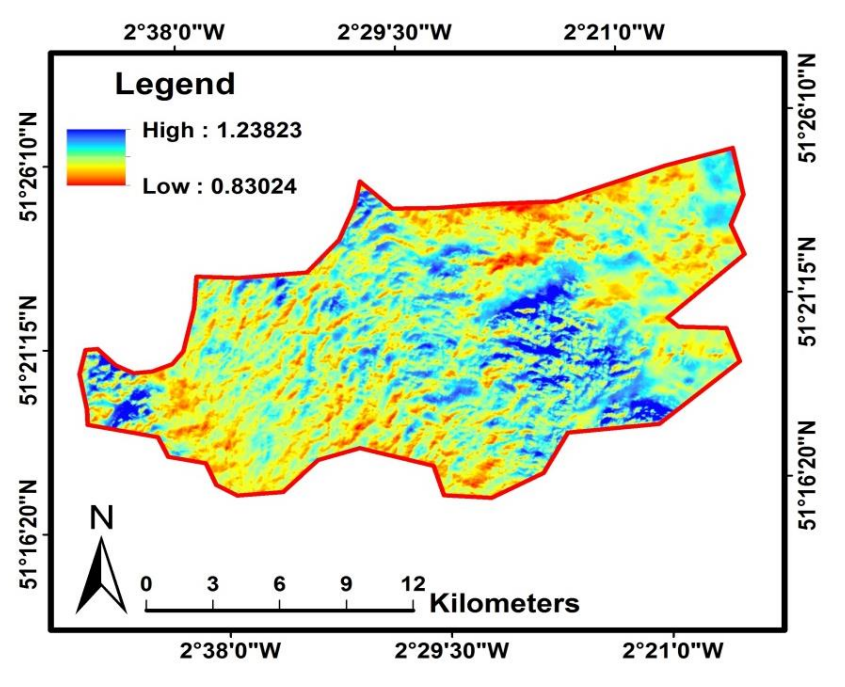


Figure 5: WRI value of Bath as extracted from Landsat 8 OLI

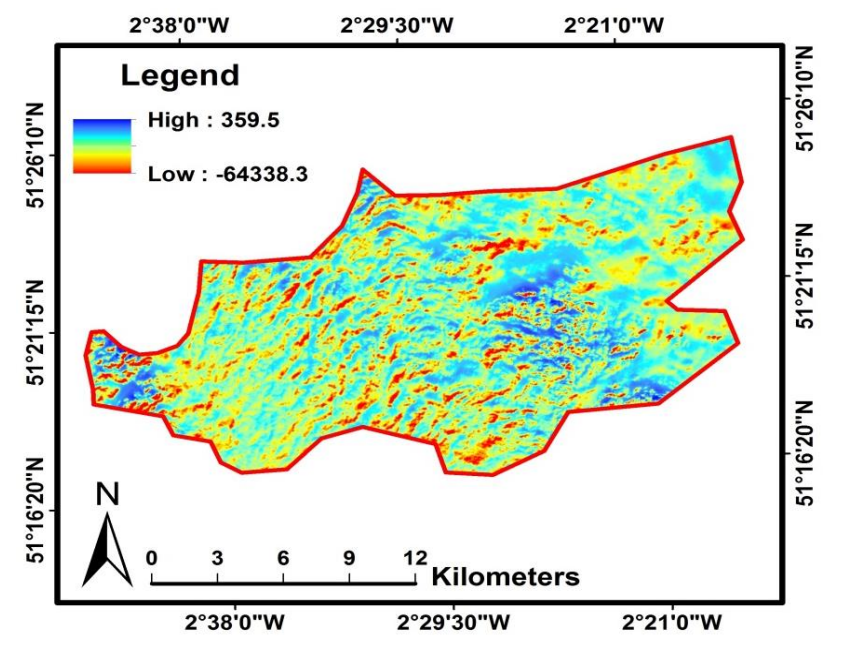


Figure 6: AWEI nsh value of Bath as extracted from Landsat 8 OLI

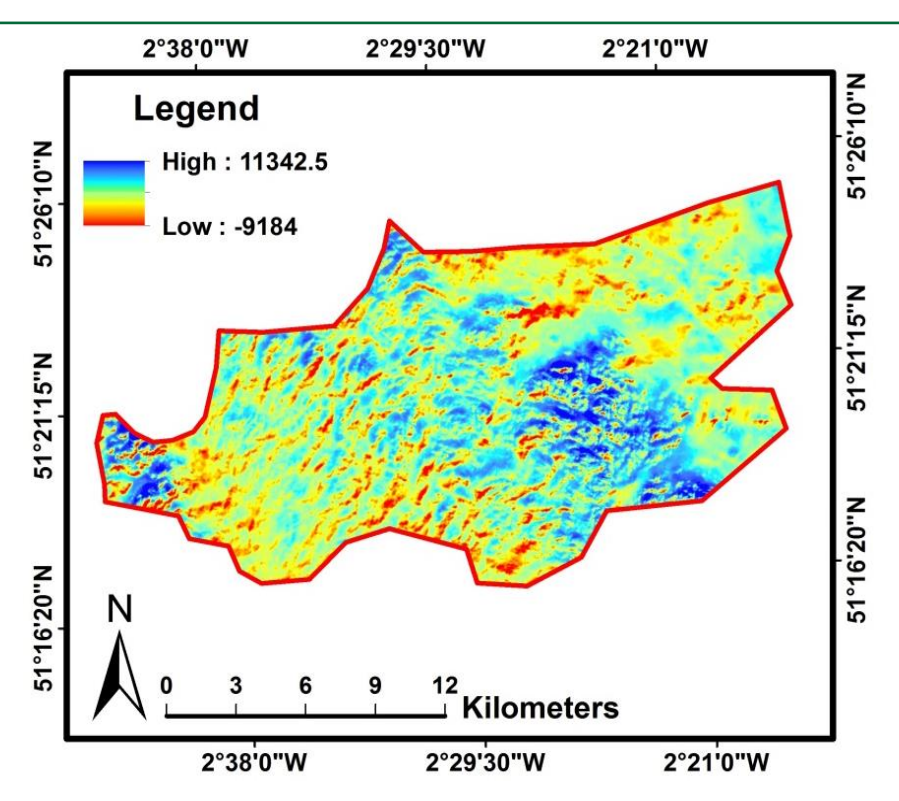


Figure 7: AWEI sh value of Bath as extracted from Landsat 8 OLI

The Water Ratio Index (WRI) serves to estimate soil or vegetation water content. It is calculated by dividing the combined spectral index of green and red visible light bands by the combined spectral index of short and mid-wave infrared light bands, as detailed in Eq. (1). This index aids in determining water features within a region, with possible values ranging from 0 to 3. Typically, values exceeding one indicate the presence of water or moisture. In WRI calculation, wet objects are assigned a value of 1, effectively classifying the world into dry (no water on the surface) and wet (areas with moisture-retaining plants and water bodies). High water index values indicate wet vegetation cover and water objects, as shown in Figure 5. Bright areas in the central, eastern, and western sections likely depict fields that have been watered or encompass water bodies. A combined approach of analysis (visual identification of wet fields and classification based on specific values to identify water objects) is essential for precise image analysis.

In Eq. (2), significant positive values for water pixels arise from the contrast between band 3 and band 6, leading to negative values for most non-water pixels. Bands 5 and 7 have minimal water reflectance, hence subtracting their values with varying weights amplifies negative values for non-water pixels. Negative values for water pixels are rare in this subtraction. Fig. 6 reveals that grass-covered, soil, bright buildings, and other highly reflective surfaces for bands 5 or 7 yield large negative values in the equation's outcome. The equation aims to enhance discrimination between wet, dark, and dry surfaces (Fajar et al., 2022). While bands 5, 6, and 7 are mostly absorbed by water, bands 2 and 3 exhibit higher reflectance. Shadowed surfaces show uniform low reflectance, varying depending on shading degree and surface type. Eq. (2) alone may not fully eliminate shadows and low albedo surfaces. Fig. 6 demonstrates that removing band 6 from band 3 may yield positive water and shadow values, illustrating the challenge of excluding shadow pixels based solely on this equation.

To address these limitations, Eq. (3) was developed to enhance separation between water, shadows, and dark surfaces. As shown in Figure 7, bands 2 and 3 display significant reflectance variation between water and shadows. Combining these bands while multiplying band 3 by a coefficient increases separability, yielding positive values for water and comparatively lower values for shadows. Despite a minimal impact on water pixels, subtracting bands 5, 6, and 7 greatly affects non-water surfaces, pushing them below zero. Eq. (4) was excluded from Eqs. (2) and (3) as its inclusion did not enhance separability and accuracy in initial tests. Eq. (3) may not effectively distinguish between high albedo surfaces like ice and clouds and water due to their large positive reflectance values resulting from the inclusion of short wave bands (bands 2 and 3).

For the application of the two AWEI equations: 1) AWEI enhances the separability of water pixels from non-water, ensuring that a threshold

near zero is suitable for collecting surface water, 2) AWEI sh is suggested when shadows significantly affect accuracy; if shadows pose minimal challenge, 3) AWEI nsh is recommended. In scenarios with both high albedo surfaces and shadow/dark areas, using Eqs. (2) and (3) consecutively in a hierarchical manner is suggested. 4) In settings without shaded areas, dark urban landscapes, or high albedo surfaces, independent use of AWEI nsh is advised. As technology and remote sensing capabilities continue to advance, the Automated Water Extraction Index (AWEI) plays an increasingly important role in enhancing our understanding of water-resource interactions, guiding sustainable practices, and supporting effective decision-making in water-scarce regions.

# 5. CONCLUSIONS

This study investigated the feasibility of applying Landsat 8 OLI data from the Landsat 8 satellite to identify surface water bodies in both urban and rural contexts within the city of Bath, which is located in the United Kingdom. The remote sensing technology was used for this investigation. The major purpose was to evaluate the efficacy of extraction indices in improving the difference between water and non-water surfaces, hence improving the accuracy of water extraction. This was particularly important in regions where difficulties such as shadows and urban surroundings make exact categorization difficult. By utilizing the OLI data from Landsat 8, we were able to introduce two indices, namely the Automated Water Extraction Index (AWEI) and the Water Ratio Index (WRI), and then compare their respective performance.

Based on the data, it is clear that the Water Ratio Index (WRI) stands out as the method that is both the most effective and the most basic when it comes to extracting and mapping water resources. Even though there are indices that can make a more nuanced distinction between land and water, the World Resources Institute (WRI) is still a reliable instrument that can help guide rational decision-making. According to the Water Ratio Index, places that are struggling with water scarcity and insufficient moisture encompass vast regions. This highlights potential looming concerns that necessitate taking proactive efforts to counteract volatile environmental and climatic alterations. It was discovered that the proportion of waterrich or wet regions to total area was 1.24, which is a rather small proportion and indicates poor coverage.

Before the Automated Water Extraction Index (AWEI) was implemented, prevalent misclassifications were the consequence of pre-existing obstacles such as shadows and dark surfaces. These challenges led to the need for the AWEI. As a result, we suggest AWEI as an improved water index, particularly appropriate for extracting water data in settings defined by the presence of shadows and man-made surfaces, where it is difficult to obtain trustworthy results. AWEI has shown that it is capable

of accurate categorization of edge pixels, and the fact that it maintains a stable threshold makes it a good choice for analyzing changes in conditions near the water's surface. When it came to recognizing the presence of water, AWEI nsh values performed noticeably better than AWEI sh values. However, the AWEI nsh revealed a substantially greater detection rate, with a value of 11342.5 for these places, suggesting its enhanced accuracy. While the AWEI sh failed to identify some moist spots (highest value = 359.5), the AWEI nsh did.

These indices and thresholds, when properly selected, have the ability to efficiently isolate the specific aspects of interest from other features and can be used for change detection reasons. The application of these indices to the detection of distinct land coverings across a variety of seasons, sensor datasets, and study locations is one possible approach that future research could take.

### REFERENCES

- 100 Largest Cities and Towns in the UK by Population [Internet]. 2019. The Geographist. 4 May 2019 [updated 2023 June 10; cited 2023 June 10]. Available from: https://en.wikipedia.org/wiki/Bath\_Somerset.
- Acharya, T.D., Lee, D.H., Yang, I.T., Lee, J.K., 2016. Identification of Water Bodies in a Landsat 8 OLI Image using a J48 Decision Tree. Sensors, 16, Pp. 1075. doi:10.3390/s16071075.
- Acharya, T.D., Yang, I.T., Lee, D.H., 2017. Water Index Based Coastline Detection from Landsat Images. Conference of the Korean Society for Geospatial Information Science; May 25-26, 2017; Seoul, Korea, Pp. 187-188.
- Acharya, T.D., Yang, I.T., Subedi, A., Lee, D.H., 2017. Change Detection of Lakes in Pokhara, Nepal using Landsat Data. Proceedings, 1. doi: 10.3390/ecsa-3-E005.
- Ahmed, A., Hasan, M.K., Esha, E.J., 2017. Water Body Mapping and Monitoring using Landsat Time Series Satellite Images. Journal of Remote Sens. GIS & Technology, 3 (1), Pp. 1-16.
- Alderman, K., Turner, L.R., Tong, S.L., 2012. Floods and human health: A systematic review. Environment International, 47, Pp. 37–47. doi: 10.1016/j.envint.2012.06.003.
- Bond, N.R., Lake, P.S., Arthington, A.H., 2008. The impacts of drought on freshwater ecosystems: An Australian perspective. Hydrobiologia, 600, Pp. 3–16. doi: 10.1007/s10750-008-9326-z.
- Dambach, P., Machault, V., Lacaux, J.P., Vignolles, C., Sié, A., Sauerborn, R., 2012. Utilization of combined remote sensing techniques to detect environmental variables influencing malaria vector densities in rural West Africa. International J. of Health Geographics, Pp. 11. doi: 10.1186/1476-072X-11-8.
- Dewan, A.M., Islam, M.M., Kumamoto, T., Nishigaki, M., 2007. Evaluating flood hazard for land-use planning in Greater Dhaka of Bangladesh using remote sensing and GIS techniques. Water Res. Manag., 21, Pp. 1601–1612. doi: 10.1007/s11269-006-9116-1.
- Du, Z., Bin, L., Ling, F., Li, W., Tian, W., Wang, H., Gui, Y., Sun, B., Zhang, X., 2012. Estimating surface water area changes using time-series Landsat data in the Qingjiang River Basin, China. Journal of Applied Remote Sens., 6 (1), Pp. 063609. doi: 10.1117/1.JRS.6.063609.
- Elsahabi, M., Negm, A., El Tahan, A.H.M., 2016. Performances evaluation of surface water areas extraction techniques using Landsat ETM+ data: case study Aswan High Dam Lake (AHDL). Procedia Techno., 22, Pp. 1205-1212. doi: 10.21608/eijest.2016.97140.
- Fajar, Y., Dony, K., Syarif, B., Gatot, N., Galdita, A.C., Esthi, K.D., Anjar, I.P., 2022. Evaluation of the Threshold for an Improved Surface Water Extraction Index Using Optical Remote Sensing Data. The Scientific World J., Pp. 1-19. doi.org/10.1155/2022/4894929.
- Feyisa, G.L., Meilby, H., Fensholt, R., Proud, S.R., 2014. Automated Water Extraction Index: A new technique for surface water mapping using Landsat imagery. Remote Sens. of Enviro., 140, Pp. 23-35. doi: 10.1016/j.rse.2013.08.029.
- Gautam, V.K., Gaurav, P.K., Murugan, P., Annadurai, M., 2015. Assessment of Surface Water Dynamicsin Bangalore Using WRI, NDWI, MNDWI, Supervised Classification and KT-Transformation. Aquatic Procedia, 4, Pp. 739-746. doi: 10.1016/j.aqpro.2015.02.095.

- Giardino, C., Bresciani, M., Villa, P., Martinelli, A., 2010. Application of remote sensing in water resource management: The case study of Lake Trasimeno, Italy. Water Res. Management, 24, Pp. 3885–3899. doi: 10.1007/s11269-010-9639-3.
- Guttler, F.N., Niculescu, S., Gohin, F., 2013. Turbidity retrieval and monitoring of Danube Delta waters using multi-sensor optical remote sensing data: An integrated view from the delta plain lakes to the western-northwestern Black Sea coastal zone. Remote Sens. of Enviro., 132, Pp. 86–101. doi: 10.1016/j.rse.2013.01.009.
- He, B., Oki, K., Wang, Y., Oki, T., Yamashiki, Y., Takara, K., 2012. Analysis of stream water quality and estimation of nutrient load with the aid of Quick Bird remote sensing imagery. Hydro. Sciences J. Des Sciences Hydrologiques, 57, Pp. 850–860. doi: 10.1080/02626667.2012.683792.
- Jain, S.K., Saraf, A.K., Goswami, A., Ahmad, T., 2006. Flood inundation mapping using NOAA AVHRR data. Water Res. Manag., 20, Pp. 949– 959. doi: 10.1007/s11269-006-9016-4.
- Jain, S.K., Singh, R.D., Jain, M.K., Lohani, A.K., 2005. Delineation of flood-prone areas using remote sensing technique. Water Res. Manag., 19, Pp. 337–347. doi: 10.1007/s11269-005-3281-5.
- Ji, L., Zhang, L., Wylie, B., 2009. Analysis of dynamic thresholds for the normalized difference water index. Photogrammetric Eng. and Remote Sens., 75, Pp. 1307–1317. doi: 10.14358/PERS.75.11.1307.
- Jiang, Z., Qi, J., Su, S., Zhang, Z., Wu, J., 2012. Water body delineation using index composition and HIS transformation. International J. of Remote Sens., 33, Pp. 3402–3421. doi: 10.1080/01431161.2011.614967.
- Karpatne, A., Khandelwal, A., Chen, X., Mithal, V., Faghmous, J., Kumar, V., 2016. Global Monitoring of Inland Water Dynamics: State-of-the-Art, Challenges, and Opportunities. In Computational Sustainability. Lässig, J., Kersting, K. and Morik, K., Eds., Springer International Publishing: Cham, Pp. 121-147. doi: 10.1007/978-3-319-31858-5\_7.
- Kensington Meadows [Internet]. 2023. Natural England. Archived from the original on 4 March 2016 [updated 2023 June 10; cited 2023 June 10]. Available from: https://en.wikipedia.org/wiki/Bath,\_Somerset.
- Li, K.Z., Wu, S.H., Dai, E.F., Xu, Z.C., 2012. Flood loss analysis and quantitative risk assessment in China. Natural Hazards, 63, Pp. 737–760. doi: 10.1007/s11069-012-0180-y.
- Li, W., Du, Z., Ling, F., Zhou, D., Wang, H., Gui, Y., Sun, B., Zhang, X., 2013. A comparison of land surface water mapping using the normalized difference water index from TM, ETM+ and ALI. Remote Sens., 5 (11), Pp. 5530-5549. doi: 10.3390/rs5115530.
- Lira, J., 2006. Segmentation and morphology of open water bodies from multispectral images. International J. of Remote Sens., 27, Pp. 4015–4038. doi: 10.1080/01431160600702384.
- Lu, S., Wu, B., Yan, N., Wang, H., 2011. Water body mapping method with HJ-1A/B satellite imagery. International Journal of Applied Earth Observ. and Geoinform., 13 (3), Pp. 428-434. doi:10.1016/j.jag.2010.09.006.
- McFeeters, S.K., 1996. The use of the Normalized Difference Water Index (NDWI) in the Delineation of Open Water Features. Int. J. Remote Sens., 17, Pp. 1425-1432. doi:10.1080/01431169608948714.
- Mueller, N., Lewis, A., Roberts, D., Ring, S., Melrose, R., Sixsmith, J., Lymburner, L., McIntyre, A., Tan, P., Curnow, S., Ip, A., 2016. Water observations from space: Mapping surface water from 25 years of Landsat imagery across Australia. Remote Sens. of Enviro., 174, Pp. 341-352. doi: 10.1016/j.rse.2015.11.003.
- Nath, R.K., Deb, S.K., 2010. Water-Body Area Extraction from High Resolution Satellite Images-an Introduction, Review, and Comparison. International Journal of Image Proces., 3, Pp. 353-372.
- National Research Council. 2008. Integrating multiscale observations of US waters. National Academies Press.
- Peng, Y., He, G., Wang, G., Cao, H., 2022. Surface Water Changes in Dongting Lake from 1975 to 2019 Based on Multisource Remote Sensing Images. Remote Sens., 13, Pp. 1827. doi: 10.3390/rs13091827.
- Prigent, C., Papa, F., Aires, F., Jimenez, C., Rossow, W.B., Matthews, E., 2012.

- Changes in land surface water dynamics since the 1990s and relation to population pressure. Geophys. Res. Letters, 39, Pp. L08403. doi:10.1029/2012GL051276, 2012.
- Proud, S.R., Fensholt, R., Rasmussen, L.Y., Sandholt, I., 2011. Rapid response flood detection using the MSG geostationary satellite. International J. of Applied Earth Observation and Geoinformation, 13, Pp. 536–544. doi: 10.1016/j.jag.2011.02.002.
- Published Contaminated Land Inspection of the area surrounding Bath [Internet]. 2023. Bath and North East Somerset Council. Archived from the original on 13 May 2012 [updated 2023 June 10; cited 2023 June 10]. Available from: https://en.wikipedia.org/wiki/Bath,\_Somerset.
- Rouse, J.W., Haas, R.H., Schell, J.A., Deering, D.W., 1973. Monitoring Vegetation Systems in the Great Plains with ERTS (Earth Resources Technology Satellite). In Third Earth Resources Technology Satellite Symposium, Greenbelt, ON, Canada, 10–14 December, Pp. 309-317.
- Ryu, J.H., Won, J.S., Min, K.D., 2002. Waterline extraction from Landsat TM data in a tidal flat A case study in Gomso Bay, Korea. Remote Sens. of Enviro., 83, Pp. 442–456. doi: 10.1016/S0034-4257(02)00059-7.
- Sethre, P.R., Rundquist, B.C., Todhunter, P.E., 2005. Remote detection of prairie pothole ponds in the Devils Lake Basin, North Dakota. GlScience and Remote Sens., 42, Pp. 277–296. doi: 10.2747/1548-1603.42.4.277.
- Shen, L., Li, C., 2010. Water body extraction from Landsat ETM+ imagery using adaboost algorithm. In Geoinformatics, 18th International Conference on IEEE, Pp. 1-4. doi: 10.1109/GEOINFORMATICS.2010.5567762.

- Sivanpillai, R., Miller, S.N., 2010. Improvements in Mapping Water Bodies using ASTER Data. Ecolog. Informatics, 5, Pp. 73-78. doi: 10.1016/j.ecoinf.2009.09.013.
- South West England: climate [Internet]. 2023. Met Office. Archived from the original on 25 February 2006 [updated 2023 June 10; cited 2023 June 10]. Available from: https://en.wikipedia.org/wiki/Bath\_Somerset.
- Sun, F., Sun, W., Chen, J., Gong, P., 2012. Comparison and improvement of methods for identifying waterbodies in remotely sensed imagery. International Journal of Remote Sensing, 33, Pp. 6854–6875. doi: 10.1080/01431161.2012.692829.
- Tri, D.A., Dong, H.L., In, T.Y., Jae, K.L., 2016. Identification of Water Bodies in a Landsat 8 OLI Image Using a J48 Decision Tree. Sensors, 16 (1075), Pp. 1-16. doi:10.3390/s16071075.
- Tulbure, M.G., Broich, M., 2013. Spatiotemporal Dynamic of Surface Water Bodies using Landsat Time-Series Data from 1999 to 2011. ISPRS Journal of Photogr. and Remote Sens., 79, Pp. 44-52. doi: 10.1016/j.isprsjprs.2013.01.010.
- Verpoorter, C., Kutser, T., Tranvik, L., 2012. Automated mapping of water bodies using Landsat multispectral data. Limnology and Oceanography-Methods, 10, Pp. 1037–1050. doi: 10.4319/lom.2012.10.1037.
- Xu, H., 2006. Modification of normalised difference water index (NDWI) to enhance open water features in remotely sensed imagery. International J. of Remote Sens., 27, Pp. 3025–3033. doi: 10.1080/01431160600589179.

